

Esophageal Reconstruction with ECM and Muscle Tissue in a Dog Model

Stephen F. Badylak, D.V.M., Ph.D., M.D.,*¹ David A. Vorp, Ph.D.,* Alan R. Spievack, M.D.,†
Abby Simmons-Byrd, R.V.T.,† Joseph Hanke,* Donald O. Freytes, M.S.,* Anil Thapa, M.S.,‡
Thomas W. Gilbert,* and Alejandro Nieponice, M.D.*

*McGowan Institute for Regenerative Medicine, University of Pittsburgh, Pittsburgh, Pennsylvania; †ACell, Inc., West Lafayette, Indiana; ‡Resodyn Corporation, Butte, Montana

Submitted for publication December 13, 2004

An *in vivo* study was conducted to determine if an extracellular matrix (ECM) scaffold co-localized with autologous muscle tissue could achieve constructive remodeling of esophageal tissue without stricture. ECM derived from the porcine urinary bladder was processed, decellularized, configured into a tube shape, and terminally sterilized for use as a bioscaffold for esophageal reconstruction in a dog model. Twenty-two dogs were divided into four groups, three groups of five and one group of seven. Groups 1 and 2 were repaired with either ECM alone or muscle tissue alone, respectively. Groups 3 and 4 were repaired with ECM plus either a partial (30%) covering with muscle tissue or a complete (100%) covering with muscle tissue, respectively. Animals in groups 1 and 2 were sacrificed within approximately 3 weeks because of the formation of intractable esophageal stricture. Four of five dogs in group 3 and six of seven dogs in group 4 were survived for 26 days to 230 days and showed constructive remodeling of esophageal tissue with the formation of well organized esophageal tissue layers, minimal stricture, esophageal motility, and a normal clinical outcome. Mechanical testing of a subset of the remodeled esophageal tissue from animals in groups 3 and 4 showed progressive remodeling from a relatively stiff, non-compliant ECM tube structure toward a tissue with near normal biomechanical properties. We conclude that ECM bioscaffolds plus autologous muscle tissue, but not ECM scaffolds or muscle tissue alone, can facilitate the *in situ* reconstitution of structurally and functionally acceptable esophageal tissue. © 2005 Elsevier Inc. All rights reserved.

¹ To whom correspondence and reprint requests should be addressed at McGowan Institute for Regenerative Medicine, 100 Technology Drive, Suite 200, Pittsburgh, PA 15219. E-mail: badylaks@upmc.edu.

Key Words: extracellular matrix; urinary bladder matrix; esophagus; surgery; tissue engineering; scaffold; esophageal cancer; regenerative medicine; bioscaffold.

INTRODUCTION

Surgical resection or ablation of the esophagus as a consequence of congenital or acquired disease is associated with high morbidity and a variety of potential post-surgical complications [1–5]. The esophagus has little redundancy and therefore autologous tissue for reconstruction usually is non-existent. Interpositional tubular reconstruction procedures for even small segmental defects of the esophagus have used autologous stomach tissue, small and large intestine, or skin. Complication rates for such procedures are high, ranging from 30 to 40% [6–8] and are a major concern when considering a radical esophagectomy [4]. It has been shown that the technical-related complications (e.g., leaks, bleeding) are an independent risk factor of prognostic outcome [9]. Furthermore, up to 50% of patients require postoperative dilations at the level of the cervical anastomosis after radical esophagectomy [4]. Palliative procedures, stent-like devices, and multiple bypasses have been designed for the treatment of malignant and severe benign disease in an attempt to mitigate problems with autologous graft procedures [10–13]. Stated differently, there is a need for effective strategies and methods for esophageal repair and reconstruction.

Barrett's esophagus represents metaplasia of esophageal epithelial cells and is a condition associated with an approximately 1% incidence of adenocarcinoma [14–16]. The incidence of this neoplasia is rising more rapidly than any other type of cancer and is associated

with a 5 to 10% 5-year survival rate when not treated in the very early stages [4, 17]. Surgical and non-surgical treatment options currently exist for Barrett's esophagus (BE) with high-grade dysplasia (HGD), including esophageal resection, endoscopic mucosal resection (EMR), and photodynamic therapy (PDT) [14, 18–21]. EMR is a promising approach, but some patients still require multiple endoscopic sessions to achieve a complete resection and the stricture rate is significantly increased when the resection is longer than 30 mm or greater than three-quarters of the circumference [22, 23]. Although PDT is not as strongly associated with stricture as EMR, it can require several treatment sessions and requires rigid screening protocols that make the cost-effectiveness of this procedure controversial [24]. The persistence of metaplastic glands below the neopithelial layer in the long term follow-up make PDT a questionable cancer prevention method [25, 26]. If a complete resection for EMR or a deep ablation for PDT could be achieved without stricture, this might lead to a more desirable outcome in a single endoscopic session. The cause of esophageal stricture formation is not known with certainty, but a convincing body of evidence implicates a role for molecular mediators of inflammation that lead to tissue injury, cell death, and healing by scar tissue formation.

Tissue engineering/regenerative medicine approaches that use the principles of developmental biology, cell biology, biomaterials, and medicine toward the goal of reconstituting normal tissue have not been extensively investigated for esophageal applications. *In vitro* attempts to reconstruct esophageal tubes from collagen, fibroblasts, and smooth muscle cells have been partially successful but *in vivo* translation of these techniques for forming engineered esophageal constructs has not been reported [27–29]. The use of extracellular matrix (ECM) derived from the small intestinal submucosa (SIS) and urinary bladder has shown success in pre-clinical and clinical applications for the reconstruction of numerous body structures including the lower urinary tract [30–33], vasculature [34–36], skin [37, 38], and tendons and ligaments [39, 40]. Promising results were obtained when ECM bioscaffolds were used for the replacement of partial (<50%) circumferential resection of the esophagus in a dog model [41]. One of the apparent requirements for the reconstruction of structurally and functionally normal esophageal tissue appeared to be the presence of adequate amounts of autologous muscle tissue in contact with the abluminal portion of the ECM scaffold at the time of implantation [41]. The objective of the present study was to evaluate the structural, functional, and biomechanical properties of full circumferential esophageal tissue following experimental segmental resection and reconstruction

with either an ECM scaffold alone, muscle tissue alone, or combinations of ECM plus muscle tissue.

MATERIALS AND METHODS

Overview of Experimental Design

Twenty-two adult healthy female mongrel dogs weighing between 17 and 24 kg were divided into four groups, three groups of five and one group of seven dogs. Each dog was subjected to surgical resection of 5 cm of the full circumferential esophageal endomucosa in the mid-cervical region. The endomucosa was defined as the epithelium, basal lamina (basement membrane), lamina propria, muscularis mucosa (all of which constitute the tunica mucosa), plus the tunica submucosa. Therefore, endomucosal resection left only the muscularis externa intact. The groups varied by the amount of skeletal muscle tissue that was subsequently removed from the outer muscular covering of the operated esophageal segment and by the placement or lack of placement of an ECM scaffold as a tubular graft in place of the removed endomucosa. The measured endpoints included esophageal function, morphological characteristics and, in a subset of animals, biomechanical properties of esophageal tissue.

The dogs in group 1 ($n = 5$) were subjected to resection of the complete thickness of the esophageal segment (i.e., endomucosa plus muscularis externa) and replacement of the missing esophagus with a tubularized form of an ECM bioscaffold derived from the porcine urinary bladder. The dogs in group 2 ($n = 5$) were subjected to removal of the endomucosa but the native muscularis externa was left intact (i.e., the complete endomucosa was removed but no ECM scaffold was placed). The dogs in group 3 ($n = 5$) were subjected to complete resection of the entire endomucosa and replacement of the endomucosa with an ECM tube scaffold. Seventy percent of the complete thickness of the muscularis externa was then removed and three narrow strips comprising approximately 30% of the native muscularis externa skeletal musculature was left intact. The dogs in group 4 ($n = 7$) were subjected to resection of the entire endomucosa and replacement of the endomucosa with an ECM tube scaffold. One hundred percent of the native muscularis externa skeletal musculature was left intact. Figure 1 depicts the layers of esophagus that were removed during these surgical procedures. Table 1 summarizes treatment of the study groups. The dogs were survived until stricture formed that prevented swallowing (typically within 14–21 days) or were electively euthanized at a later time if intractable stricture did not occur. Harvested tissue from seven of the 12 animals in groups 3 (three dogs) and 4 (four dogs) was subjected to biomechanical testing that consisted of pressure-diameter response evaluation and uniaxial tensile testing, both of which are described in detail below. Because the mechanical properties testing precluded immediate fixation for histomorphologic examination, it was decided to preserve a subset of the specimens for morphological examination only (i.e., the remaining five of 12 dogs in groups 3 and 4). The specimens subjected to mechanical properties testing were chemically fixed (10% buffered formaldehyde) for histological examination after the completion of the testing (approximately 8 h).

ECM Device Preparation

Porcine urinary bladders were harvested from market weight (approximately 110–130 kg) pigs (Whiteshire-Hamroc, IN). Residual external connective tissues, including adipose tissue, were trimmed and all residual urine removed by repeated washes with tap water. The urothelial layer was removed by soaking of the material in 1 N saline. The tunica serosa, tunica muscularis externa, and the tunica submucosa were mechanically delaminated from the remaining bladder tissue. The remaining basement membrane of the tunica mucosa and the subjacent tunica propria, collectively termed urinary bladder matrix (UBM), were then isolated and disinfected by immersion in 0.1% (v/v) peracetic acid (σ), 4% (v/v) ethanol, and 96% (v/v) sterile

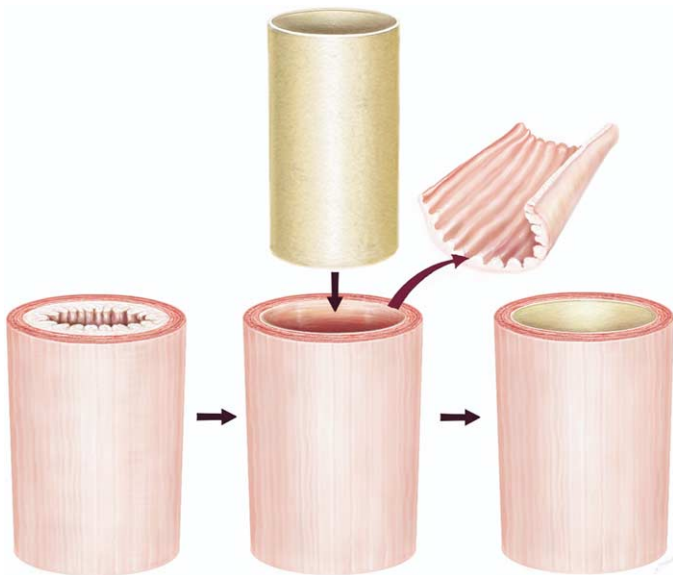


FIG. 1. Graphic representation of a segment of esophagus in which the endomucosa was removed (middle figure) and replaced by a tubularized form of ECM. In the present study, the construct depicted on the right hand side of this figure would be equivalent to the procedure performed on the dogs in group 4.

water for 2 h. The UBM-ECM material was then washed twice for 15 min with PBS (pH = 7.4) and twice for 15 min with deionized water.

Multilayer tubes were created by wrapping hydrated sheets of UBM around a 30 mm perforated tube/mandrel that was covered with umbilical tape for a total of four complete revolutions (i.e., a four layer tube). This construct was placed into a plastic pouch and attached to a vacuum pump (Leybold, Export, PA, Model D4B) with a condensate trap in line. The construct was subjected to a vacuum of 28 to 29 in Hg for 10 to 12 h to remove the water and form a tightly coupled four-layer laminate. Each device was then removed from the mandrel and terminally sterilized with ethylene oxide (Fig. 2).

Surgical Procedure

Each animal was anesthetized by intravenous administration of thiopental sodium and a surgical plane of anesthesia was main-

TABLE 1

Surgical Procedures Performed on Each Group of Dogs

Group no. (n value)	Surgical procedure
1 (n = 5)	Segmental resection of full thickness esophagus, replacement with ECM scaffold.
2 (n = 5)	Segmental removal of full circumference endomucosa, muscularis externa left intact, no ECM scaffold.
3 (n = 5)	Segmental removal of full circumference endomucosa, plus 70% of muscularis externa. ECM scaffold used to replace endomucosa.
4 (n = 7)	Segmental removal of full circumference endomucosa. ECM scaffold used to replace endomucosa.



FIG. 2. Photograph of a single layer sheet of ECM following decellularization. The insert (lower right) shows a tubularized, four layer construct that has been vacuum pressed as described in the text.

tained by intubation and inhalation of Isoflurane in oxygen. The neck was shaved and the site prepared for aseptic surgery. A ventral midline approach was made and after standard draping, the skin was incised and the esophagus isolated. In group 1, a 5-cm full circumferential defect including all layers of the esophagus was created, and the defect was repaired with an interpositional placement of the ECM bioscaffold tube alone. In groups 2 to 4, a 7-cm longitudinal incision was made on the ventral surface of the esophagus, and the endomucosa of a 5 cm length of the esophagus (full circumference) was removed from all animals. Group 2 was a control group. No ECM bioscaffold was placed in the dogs in group 2. The dogs in group 3, strips of muscle from the outer muscular tube were removed in addition to the entire circumference of the endomucosa. The amount of muscle removed approximated 70% of the total circumference of the muscular tube, leaving three strips of muscle at approximately the 2, 6, and 10 o'clock positions. A tubularized ECM bioscaffold was then placed at the site of the original endomucosa in the group 3 animals. Finally, in dogs in group 4, the entire circumference of the endomucosa was removed, and a tubularized ECM scaffold was then placed at the site of the original endomucosa, leaving 100% of the abluminal muscle tube intact and in place. The ECM device in all cases was sutured to the native endomucosa at each end with 5-0 Prolene. The muscle and subcutaneous tissues were closed with 4-0 vicryl and skin was closed with skin staples.

Post-Surgical Care

The dogs were recovered from anesthesia, extubated and monitored in the recovery room until they were resting comfortably in sternal position. The dogs were kept in a cage overnight and returned to their larger run housing on postoperative day one. The dogs were given prophylactic antibiotics consisting of Cephalothin/Cephalexin 35 mg/kg, bid x 7 to 9 days. After surgery the dogs received Acepromazine (0.1 mg/kg IV) and Butorphanol (0.05 mg/kg IV), followed by Buprenorphine (0.01–0.02 mg/kg, SC or IM q 12 h) thereafter for analgesia as needed. Dogs were fed from an elevated/raised platform. The dog's daily nutrition was calculated and divided into 2 to 3 feedings per day. Gruel/soft food was provided for 1 week post-surgery. The animals were reintroduced to solid food over a 2 to 3 week period. The dogs were weighed weekly and housed in a run measuring approximately 10 × 14 ft to allow freedom to ambulate.

Endoscopic examinations and barium esophagrams were completed at approximately monthly intervals to evaluate esophageal structure and function.

Morphological Examination

Immediately after euthanasia, the cervical esophagus was harvested. The harvested tissue included the scaffold placement site plus native esophageal tissue both proximal and distal to the graft site. The excised esophagus was opened by making a longitudinal incision in the distal to proximal direction. The exposed mucosal surface was examined and the inner circumference of the esophagus measured. The tissue was then immersed in 10% neutral buffered formalin, trimmed, sectioned, and stained with both Hematoxylin and Eosin and Masson's Trichrome stains. The areas examined included the native esophagus, the proximal and distal anastomoses, and the mid-scaffold region.

Biomechanical Testing

Pressure—Diameter Responses

Immediately after euthanasia, the intact esophagus from seven animals in groups 3 and 4 was isolated and a custom clamping device [42] was used to maintain the *in vivo* length. The esophagus was excised in its entirety and was placed in lactated Ringer's solution at 4°C until time for testing (2–4 h). The esophagus was secured to stainless steel cannulae with 4-0 sutures and restored to its *in vivo* length inside an *in vitro* pressure-diameter testing system, which was modified from an *ex vivo* vascular perfusion apparatus system previously described [43, 44]. The mounted esophagus was enclosed within an 800 ml bathing chamber, the temperature of which was maintained at 37°C using a heated circulating saline loop. A laser micrometer (Beta Lasermike Model 162, Dayton, OH) was positioned orthogonal to the sample to measure the outer diameter (OD). Diameter measurements were obtained 10 and 5 mm into the native tissue direction and 5 mm into the scaffold direction from the proximal anastomosis. An adjustable height reservoir was used to translate hydrostatic pressure into transmural pressure as previously described [43, 44]. The specimens were first pre-conditioned by cycling between 0 and 9 mmHg 10 times with 10 s per cycle. After pre-conditioning, pressure-diameter responses were determined for each of the three locations by increasing the intraluminal pressure from 0 to 30 mmHg in 3 mmHg increments. The OD for each pressure was recorded and was normalized to the OD value at 0 mmHg. Compliance (C) was calculated as:

$$C = \left(\frac{OD_{12} - D_o}{D_o} \right) \frac{1}{P_{12} - P_o} \quad (1)$$

where OD_{12} is the OD at 12 mmHg and D_o is the OD at the reference pressure P_o (0 mmHg). Although the pressure-diameter response was measured up to 30 mmHg, compliance was only measured up to 12 mmHg because of changes in the shape of the pressure-diameter curve at this point, which in some cases led to diameters outside the range of the laser micrometer. For comparison, the compliance of the graft was normalized by the compliance of the native esophagus.

Tensile Testing

Test specimens were prepared by cutting the tissue into flat rectangular pieces (4 cm × 1 cm) with longitudinal or circumferential axis orientation. Additional test specimens were obtained from a piece of scaffold material before implantation as a Time Zero control. Each specimen was equilibrated to room temperature by immersion in fresh saline before biomechanical testing. The specimens were

mounted in a previously described uniaxial tensile testing apparatus [45] and continuously wetted with saline.

The uniaxial tensile testing system consisted of a rail table with a computer-interfaced microstepping motor (Model S57-83; Parker Hannifin Corporation, Compumotor, Rohmert Park, CA) [45]. The tees that held the clamped specimen were supported by two brackets and these tees moved in opposite directions during the testing procedure. A 25-lb tension load cell (Model 311430-04; Sensotec, Columbus, OH) was mounted at one end of the mounting brackets and the output magnified by an amplifier (Model SA-BII; Sensotec, Columbus, OH). An A/D converter (Model DT2801; Data Translations, Marlborough, MA) was used to digitize the load cell and output at 5 Hz, and the data were subsequently stored on a dedicated computer. To ensure that the specimen did not slip from the clamp, a small amount of cyanoacrylate glue was used between the specimen and the face of the clamp as previously done for other tissues [46]. A pre-load of 0.05 N was applied to each specimen before testing. The thickness and width of each specimen were measured at three different positions using a dial caliper. The average width and average thickness was used to calculate an initial cross sectional area for the specimen. Each specimen was preconditioned by cyclically loading it to 7% strain at a constant strain rate of 8.5%/min for 10 cycles. Following pre-conditioning, the specimen was stretched from its initial gauge length until failure at a strain rate of 8.5%/min. The change in specimen length was related to the recorded load using the known strain rate and the initial gauge length.

From the recorded load, elongation, and initial cross-sectional area, stress (σ) and strain (ϵ) were computed as follows [46]:

$$\epsilon = \frac{\Delta l}{l_o} \quad (2)$$

$$\sigma = \frac{f}{a_o} (1 + \epsilon) \quad (3)$$

where f is the force recorded by the transducer, a_o is the original cross-sectional area, Δl is the change in length associated with each force, and l_o is the original length of the specimen. The ultimate tensile strength (UTS) was taken as the peak stress attained before specimen failure. From the stress *versus* strain curve, the maximum tangential modulus (MTM) was computed. For comparison, the tangent modulus and ultimate tensile strength for the remodeled graft were normalized to those for the native esophagus.

RESULTS

The surgical procedure was successfully completed in all dogs and there was an uneventful immediate post-operative course. All five animals in group 1 (ECM scaffold alone) and group 2 (muscle alone with no ECM scaffold) developed severe esophageal stricture within approximately 3 weeks. Four of five dogs in group 3 (ECM scaffold with 30% skeletal muscle) showed constructive remodeling of the scaffold with the development of an organized, laminated tissue structure. Six of seven dogs in group 4 (ECM scaffold with 100% skeletal muscle) showed constructive remodeling of the scaffold with similar organized, differentiated tissue layers as was found in group 3. The results of this study are summarized in Table 2.

TABLE 2

Summary of Treatment Outcome and Survival Time for All Dogs in the Study

Group No.	Treatment	Survival time (days)	Outcome
1	ECM scaffold alone	14	Stricture
1	ECM scaffold alone	17	Stricture
1	ECM scaffold alone	19	Stricture
1	ECM scaffold alone	15	Stricture
1	ECM scaffold alone	13	Stricture
2	Muscle alone	21	Stricture
2	Muscle alone	27	Stricture
2	Muscle alone	15	Stricture
2	Muscle alone	20	Stricture
2	Muscle alone	19	Stricture
3	ECM scaffold + 30% muscle	72	Remodeled
3	ECM scaffold + 30% muscle	101	Remodeled
3	ECM scaffold + 30% muscle	104	Remodeled
3	ECM scaffold + 30% muscle	91	Remodeled
3	ECM scaffold + 30% muscle	26	Stricture
4	ECM scaffold + 100% muscle	180	Remodeled
4	ECM scaffold + 100% muscle	230	Remodeled
4	ECM scaffold + 100% muscle	144	Remodeled
4	ECM scaffold + 100% muscle	104	Remodeled
4	ECM scaffold + 100% muscle	217	Remodeled
4	ECM scaffold + 100% muscle	36	Stricture
4	ECM scaffold + 100% muscle	125	Remodeled

Endoscopic and Positive Contrast Examination Results

Endoscopic examination of the dogs in groups 1 and 2 showed progressive stricture with inability to pass the endoscope (six French) beyond the proximal suture line after approximately 10 days post-surgery. The operated segment developed an irregular mucosal covering with scattered foci of glistening, shiny surface mixed with reddened eroded surface by approximately 7 days post-surgery.

The endoscopic examination of dogs in groups 3 and 4 showed the rapid formation of a normal appearing mucosal surface by approximately 14 days post-surgery. The anastomotic sites in approximately 50% of the animals showed evidence of scarring with a dense white connective tissue that differed from that of either the native esophagus or the mid-scaffold region. In animals that were survived beyond 2 months post-surgery, there was obvious esophageal motility in the remodeled scaffold area as evidenced by active contraction of the esophageal tissue during endoscopic examination of the remodeled region and during visualization of the positive contrast esophagrams. No evidence for active inflammation, erosion, scarring, or necrosis was seen by endoscopic examination of the esophagus of animals from groups 3 or 4.

Positive contrast esophagrams in the animals in groups 1 and 2 showed progressive stricture with very limited passage of the barium beyond the proximal anastomotic line after approximately 2 weeks post-

surgery. The positive contrast studies in the animals in groups 3 and 4 showed passage of the positive contrast material with motility of the graft region after approximately 2 to 3 months. However, the motility of the remodeled graft tissue did not appear to be synchronous with the adjacent native esophageal tissue.

Clinical Outcomes

The animals in groups 1 and 2 showed frequent regurgitation after eating beginning on approximately post-surgery day 10. When maintenance of normal hydration became necessary by parenterally administered fluids, the animals were euthanized. The animals in all groups were fed from an elevated position during the first 3 weeks post-surgery but then resumed normal eating posture (from a bowl placed on the floor) after 3 weeks. The four animals in group 3 and the six animals in group 4 that showed constructive remodeling of the esophageal tissue had normal appetites and were eating a normal consistency food by 3 weeks post-surgery. All of these animals showed normal hydration, normal weight, and normal activity.

Macroscopic Appearance

The animals in groups 1 and 2 uniformly showed esophageal stricture formation within a period of time ranging from 13 to 19 days (group 1) and 15 to 27 days (group 2). The tissue showed an esophageal luminal circumference that was less than 20% of the adjacent normal esophageal luminal circumference (Fig. 3). The tissue was very firm to the touch. The mucosal surface within the surgically manipulated area was reddened, irregular in contour, and showed only patches of white,



FIG. 3. Macroscopic view of animal in group 1 that survived for 19 days and developed an intractable stricture. Native esophagus can be seen at the bottom of the photograph and the prolene suture material identifies the anastomosis separated from the site of ECM scaffold placement.



FIG. 4. Macroscopic appearance of remodeled ECM scaffold when skeletal muscle cells were present on the abluminal surface. This tissue was removed from an animal in group 3 and shows the area of bioscaffold remodeling with minimal narrowing of the lumen. However, note the lack of rugal folds in the esophageal mucosa. This animal had normal eating habits, gained weight throughout the post-operative period, and showed no adverse clinical signs.

normal appearing mucosal tissue. The length of the operated esophageal segment in these animals had shortened to less than 50% of the original 5-cm length.

The remodeled ECM graft in the animals in groups 3 and 4 showed similar morphological characteristics to each other. The length of the grafts was approximately 90% of the original 5 cm length, and the luminal surface appeared to contain a normal mucosal covering (Fig. 4). Examination of the cross-sectional surface showed a well-delineated outer muscular layer, a sub-mucosal layer, and a mucosal layer (Fig. 5). The luminal circumference was approximately 80% of the adjacent native esophageal luminal circumference.

Microscopic Examination

Histopathologic examination of the tissues removed from the animals in group 1 showed a lack of an intact epithelium, chronic active inflammation of the subjacent tissue characterized by an accumulation of both polymorphonuclear leukocytes and mononuclear inflammatory cells, and a variable amount of dense, disorganized, fibrous connective tissue (scarring). The ECM scaffold material had become integrated into the host tissue to the extent that it was indistinguishable from the adjacent host tissue. There was a lack of any muscular tissue in the region of the esophagus that would normally constitute the muscularis externa. The ECM scaffold was not identifiable (Fig. 6).

Histopathologic examination of the tissues in the animals in group 2 showed an intact muscularis externa. The most superficial (i.e., luminal) region of the muscularis externa was infiltrated with a mixture of

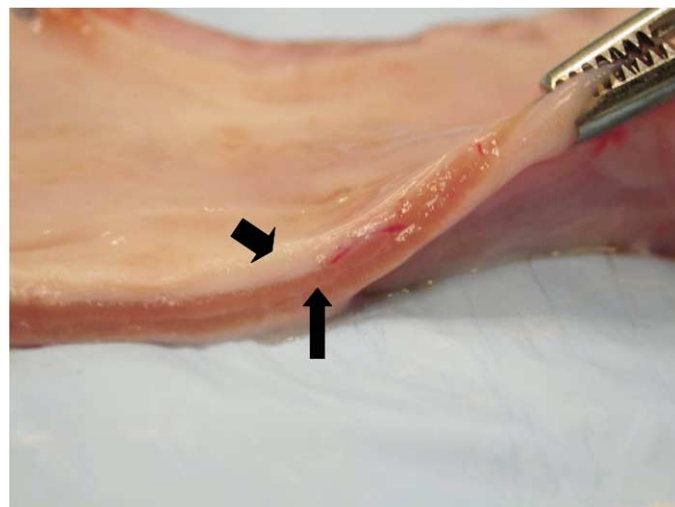


FIG. 5. Cross section of remodeled ECM bioscaffold from group 3 dog (91 day survival). Note the red area of well-organized muscle tissue (arrow) and the superficial luminal mucosal lining (arrow-head). Note also the absence of scar tissue.

inflammatory cells including polymorphonuclear leukocytes and mononuclear inflammatory cells. The tissue was very vascular and there was a lack of any intact mucosal epithelium. There were accumulations of disorganized collagenous connective tissue that represented typical scar tissue formation.

Histopathologic examination of the animals in groups 3 and 4 showed identical findings to each other. There was an intact, well-organized muscularis externa in both groups of animals. The intact circumfer-

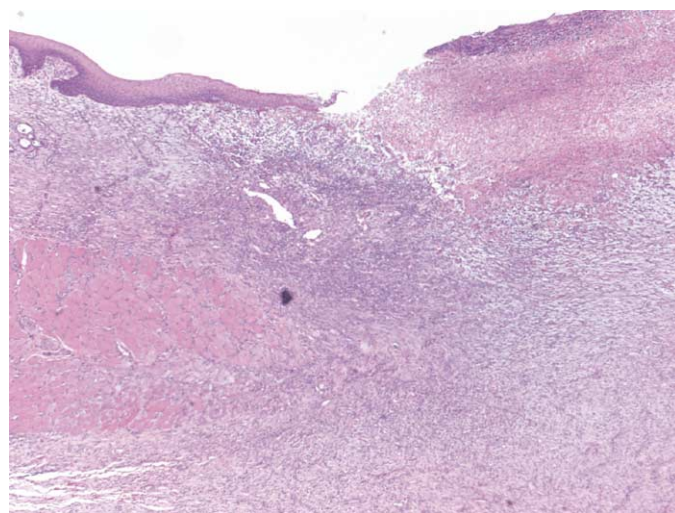


FIG. 6. Photomicrograph of a section of remodeled ECM scaffold alone (group 1) at the site of anastomosis with the adjacent native esophagus (left hand side). Remnants of skeletal muscle and squamous epithelium can be seen at the edge of the native esophageal tissue (left). The remodeled graft tissue shows a lack of squamous epithelial coverage with an underlying disorganized accumulation of fibroblastic cells and mixed inflammatory cells. This animal had developed an intractable stricture (H&E stain, $\times 20$).

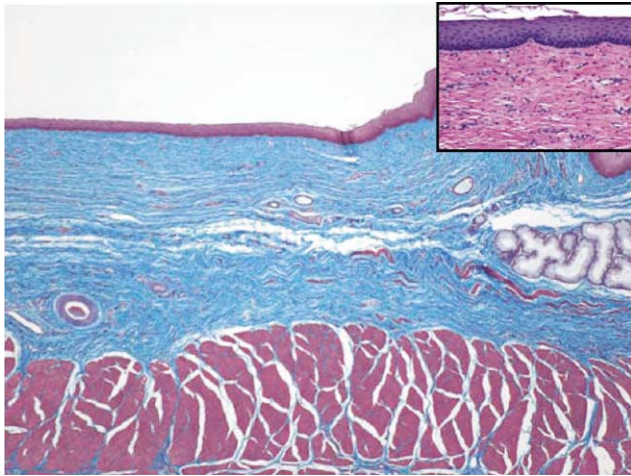


FIG. 7. Photomicrograph of remodeled ECM bioscaffold 180 days after surgery. Note the intact squamous epithelium with few rete ridges (inset), organized submucosal layer with glandular structure (right side of photograph) and organized layers of skeletal muscle in the location of the muscularis externa. Note also the lack of scar tissue formation (H&E, $\times 20$)

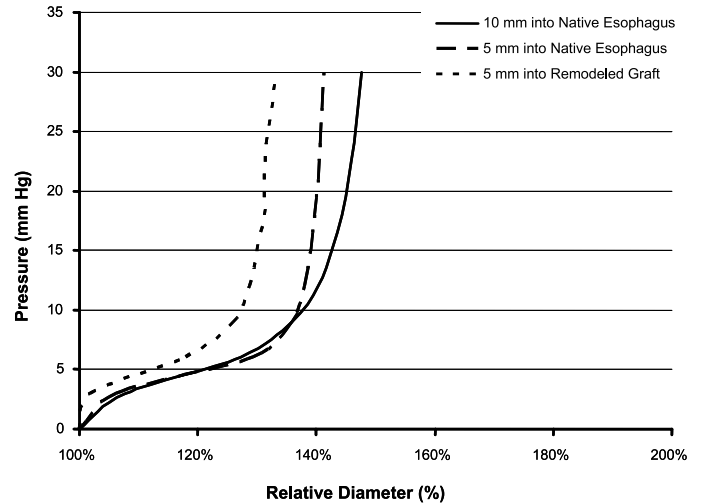


FIG. 8. Pressure-Diameter curves for native esophagus and remodeled scaffold at 145 days after surgery. The values for scaffold at 5 mm from the anastomotic site are very similar to that of native tissue. The value for the remodeled scaffold at 10 mm from the anastomotic site was not available for testing.

entail muscularis externa included the animals in group 3 in which only 30% of the native muscular layer had been retained at the time of surgery. The surface of the graft was lined by a stratified squamous epithelium upon an intact basement membrane. Rete pegs of the epithelium were not as pronounced as those in the adjacent native esophageal mucosa (Fig. 7). The submucosal tissue consisted of organized connective tissue with an abundant capillary supply. There was an absence of inflammatory cells in any of the remodeled scaffold materials that were examined beyond 3 weeks post-surgery. A moderately dense accumulation of collagenous connective tissue was present in the areas of anastomosis, especially around the remnants of suture material.

Mechanical Properties

The pressure-diameter response of the seven esophageal specimens from groups 3 and 4 had a typical shape for a muscular tube (Fig. 8). The diameter increased rapidly under low pressure and very little under higher pressure. The remodeled ECM scaffolds showed less distensibility than the native tissue until approximately 200 days after implantation when the pressure diameter response of the remodeled scaffold tissue became similar to the native esophageal tissue.

The compliance of the remodeled scaffold material and for the native esophageal tissue that was located near the anastomosis was less than for the normal esophageal tissue at the early time points and both values tended to increase to approximately that of native esophageal tissue by 100 days post-surgery (Fig. 9). The compliance was measured from 0 to 12 mmHg because the large initial OD of some of the specimens

resulted in pressurized diameters that were outside the measurement range of the laser micrometer at higher pressures.

During uniaxial tensile tests of the native tissue and remodeled graft, half of the samples failed in the mid-substance of the tissue and the other half failed at the clamp. The MTM and UTS of the graft at Time Zero were both much greater than those for the native esophagus in both the longitudinal and circumferential directions. However, by 91 days after implantation both of these properties approached those of the native esophagus and this trend continued over time (Figs. 10 and 11).

DISCUSSION

The present study showed that the use of a xenogenic ECM bioscaffold derived from porcine urinary

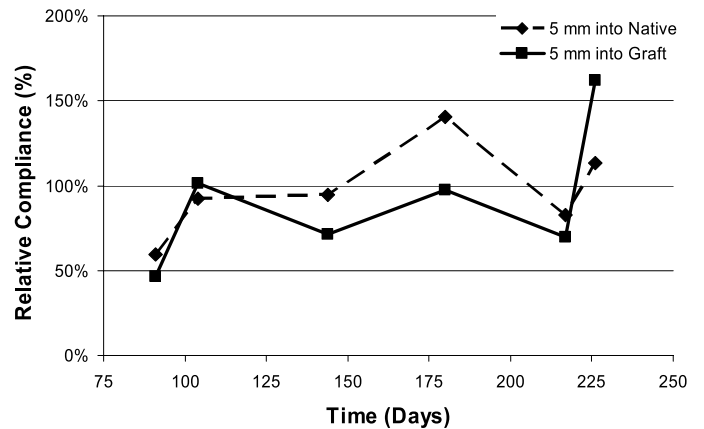


FIG. 9. Relative compliance for tissue specimens taken from 5 mm into the native esophagus and the remodeled scaffold. The compliance of normal esophageal tissue is represented by the 100% value.

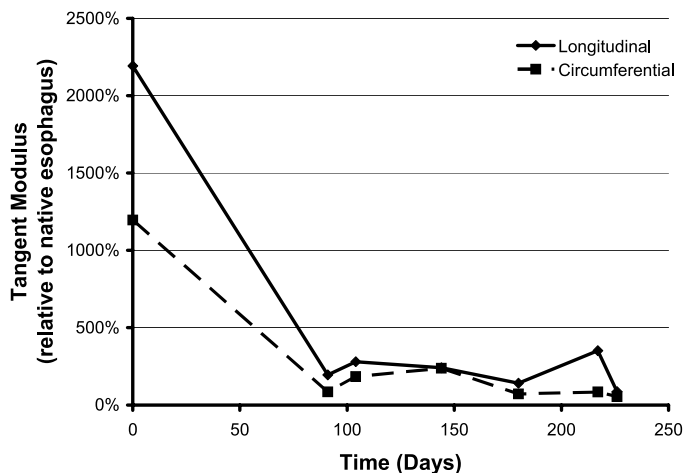


FIG. 10. MTM of the ECM graft relative to native esophagus over implant. The modulus of the graft is much greater than the native tissue initially, but rapidly remodels such that the modulus of the graft approaches that of the native esophagus (i.e., 100%) by 91 days after surgery.

bladder can induce the constructive remodeling response into functional esophageal tissue if the scaffold is placed in direct contact with autologous muscle tissue, even relatively small amounts (i.e., 30% circumference) of muscle tissue. However, use of the ECM bioscaffold alone or muscle tissue alone results in unacceptable scar tissue formation and stricture. Finally, this study showed that the mechanical behavior of the UBM scaffold changes during the remodeling process from a very stiff, relatively non-compliant state to a state in which the properties are very similar to native esophageal tissue.

The constructive remodeling response observed in the present study when an ECM bioscaffold plus muscle tissue is used for tissue reconstruction is very similar to the remodeling response seen in other body locations when ECM scaffold material has been used in tissues that contain a muscular component. For example, numerous reports of lower urinary tract reconstruction including the urinary bladder, urethra, and ureter show similar replacement of the ECM scaffold by an epithelial cell population, submucosa, and smooth muscle cell layer. In these locations, the presence of a muscle cell population in contact with the ECM scaffold enhanced but was not essential for, remodeling without scar tissue formation [47–51]. Replacement of muscular body wall structures with sheets of skeletal muscle mixed with collagenous connective tissue and adipose tissue have been reported with a porcine ECM scaffold derived from SIS [52–54].

There is a convincing body of evidence that cell to cell communication is an important determinant for constructive wound healing. Reconstruction of both dermal tissue and lower urinary tract structures show that the presence of an epithelial cell population stimulates proliferation, promotes differentiation and mi-

gration, and contributes to spatial organization of an underlying mesenchymal cell component [31, 55–57]. For example, it has been shown that the presence of urothelial cells is responsible for the differentiation of smooth muscle cell migration and differentiation in the remodeling of urinary bladder tissue [56]. Atala has shown that coculture of urothelial cells and urinary bladder smooth muscle cells not only facilitates tissue growth but significantly inhibits contraction of remodeling tissue, a finding that has direct implications to the phenomenon of esophageal stricture formation in the present study [33, 58]. In a similar fashion, squamous epithelial cells of the skin not only provide a protective covering for the underlying tissue but also provide signals that stimulate nerve cell growth and fibroblast migration and minimize fibroblast contraction of wounds [59].

It is now reasonably well accepted that complete endothelial cell coverage of vascular grafts has a marked inhibitory effect on the intimal hyperplasia that occurs during healing after vascular injury [60, 61]. Cell signaling from the overlying endothelium promotes normal organization of underlying smooth muscle cells and myofibroblasts and inhibits the excessive proliferation that is analogous to scar tissue formation and the associated wound contracture seen in other tissues and organs such as skin and the esophagus.

Finally, when considering the phenomenon of cell to cell communication *in vitro*, the feeder layer technique described by Rheinwald and Green is an excellent example of how an underlying mesenchymal cell population (NIH 3T3 fibroblasts) can have a positive effect upon the growth, migration, and proliferation of an overlying epithelial cell population [62]. The exact mechanisms of these effects are not known with cer-

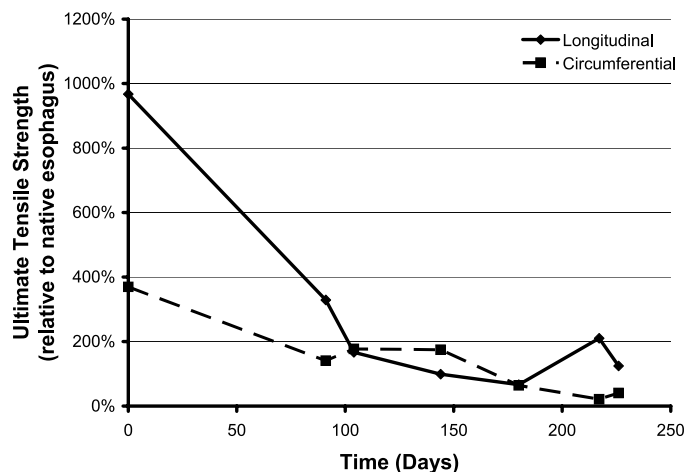


FIG. 11. UTS of the ECM graft relative to native esophagus over implant. The tensile strength of the graft is much greater than the native tissue initially, but rapidly remodels such that the strength of the graft approaches that of the native esophagus (i.e., 100%) by 91 days after surgery.

tainty, but it seems clear that site-specific cell:cell and cell:matrix signaling is a very important determinant of tissue remodeling.

ECM scaffolds that are not chemically cross-linked have been shown to have a very rapid rate of *in vivo* degradation [63–65]. Although the ECM scaffolds used in the present study were not labeled, the histological examination showed rapid loss of structural identity and rapid integration into host tissues consistent with the findings of the previous studies. This rapid rate of degradation likely contributes to the absence of a foreign body response and the associated fibrous connective tissue that is characteristic of many non-resorbable biomaterials.

The source of cells that remodel the ECM scaffold is not fully understood. It is likely that the mucosal epithelium within the remodeled scaffold area is a result of migration of cells from the adjacent native esophageal mucosa. The source of cells that contribute to the formation of a submucosal layer and the muscularis externa layer in group 3 is somewhat less clear. Recent studies with porcine derived bioscaffolds suggest that a bone marrow derived progenitor cell may participate in the remodeling of such scaffolds [66]. In addition, it has been shown that ECM scaffold degradation is an integral and necessary component of remodeling and that degradation products of the scaffold have chemoattractant properties for host endothelial cells [67]. Stated differently, the relative contribution of cells derived from adjacent native tissue *versus* a circulating population of cells to the remodeling response remains unknown.

Evaluation of the mechanical properties of remodeled esophageal tissue in the present study showed that the remodeling process progressed with time toward a tissue construct that had mechanical properties very similar to that of native tissue. The histological findings that showed progressive layered organization of the remodeled tissue were consistent with the trends observed in the mechanical properties of the remodeled tissue. Stated differently, the absence of scar tissue and the presence of an abluminal skeletal muscle cell layer, an organized, non-scarring submucosal layer, and an intact epithelium appear to support formation of a stable, functional tissue with mechanical properties similar to native esophageal tissue.

In summary, the findings of the present study suggest that it is possible to reconstruct functional full-circumferential esophageal tissue *in situ*. These findings also suggest that the observed phenomenon does not represent regeneration but rather modified wound healing response from the default scar tissue formation that is typical of adult mammalian esophageal healing. The mechanisms by which naturally occurring ECM scaffolds support such remodeling are not completely understood, but it seems clear that a combination of an

appropriate ECM microenvironment *in situ* and the presence of at least a small amount of normal host skeletal muscle cells are required for a constructive remodeling response. One limitation of the present study is that it was performed in the cervical esophagus. Pathology most commonly occurs in the distal esophagus; a location where gastric reflux may affect the healing or remodeling process. However, the promising results of the present study suggest a potential alternative treatment for conditions such as Barrett's esophagus with high-grade dysplasia, where a more aggressive resection or ablation could be attempted in a single endoscopic session. Other potential applications for ECM bioscaffolds in the esophageal location include the treatment of esophageal atresia, esophageal trauma, or other pathologies requiring resection of esophageal tissue.

REFERENCES

1. Heitmiller, R. F., Fischer, A., and Liddicoat, J. R. Cervical esophagogastric anastomosis: Results following esophagectomy for carcinoma. *Dis. Esophagus*. **12**: 264, 1999.
2. Iannettoni, M. D., Whyte, R. I., and Orringer, M. B. Catastrophic complications of the cervical esophagogastric anastomosis. *J. Thorac. Cardiovasc. Surg.* **110**: 1493, 1995; discussion 1500.
3. Luketich, J. D., Nguyen, N. T., Weigel, T., *et al.* Minimally invasive approach to esophagectomy. *JSLs* **2**: 243, 1998.
4. Orringer, M. B., Marshall, B., and Iannettoni MD. Transhiatal esophagectomy for treatment of benign and malignant esophageal disease. *World J. Surg.* **25**: 196, 2001.
5. Yildirim, S., Koksall, H., Celayir, F., *et al.* Colonic interposition vs. gastric pull-up after total esophagectomy. *J. Gastrointest. Surg.* **8**: 675, 2004.
6. Alcantara, P. S., Spencer-Netto, F. A., Silva-Junior, J. F., *et al.* Gastro-esophageal isoperistaltic bypass in the palliation of irresectable thoracic esophageal cancer. *Int. Surg.* **82**: 249, 1997.
7. Ellis, F. H., Jr. Standard resection for cancer of the esophagus and cardia. *Surg. Oncol. Clin. North. Am.* **8**: 279, 1999.
8. Gawad, K. A., Hosch, S. B., Bumann, D., *et al.* How important is the route of reconstruction after esophagectomy: A prospective randomized study. *Am. J. Gastroenterol.* **94**: 1490, 1999.
9. Rizk, N. P., Bach, P. B., Schrag, D., *et al.* The impact of complications on outcomes after resection for esophageal and gastroesophageal junction carcinoma. *J. Am. Coll. Surg.* **198**: 42, 2004.
10. Fujimaki, M. My devise for the operation of esophageal and gastric cancer. *Nippon Geka Gakkai Zasshi (in Japanese English abstract)* **98**: 786, 1997.
11. Inoue, H. Endoscopic mucosal resection for esophageal and gastric mucosal cancers. *Can. J. Gastroenterol.* **12**: 355, 1998.
12. Mayoral, W. The esophacoil stent for malignant esophageal obstruction. *Gastrointest. Encosc. Clin. North Am.* **9**: 423, 1999.
13. Watson, A. Self-expanding metal oesophageal endoprosthesis: Which is best? *Eur. J. Gastroenterol. Hepatol.* **10**: 363, 1998.
14. Fitzgerald, R. Barrett metaplasia: Reassessment of treatment and follow-up. *Curr. Opin. Oncol.* **16**: 372, 2004.
15. Murray, L., Watson, P., Johnston, B., *et al.* Risk of adenocarcinoma in Barrett's oesophagus: Population based study. *BMJ* **327**: 534, 2003.
16. Shaheen, N. J., Crosby, M. A., Bozyski, E. M., and Sandler,

- R. S. Is there publication bias in the reporting of cancer risk in Barrett's esophagus? *Gastroenterology* **119**: 333, 2000.
17. Powell, J., McConkey, C. C., Gillison, E. W., and Spychal, R. T. Continuing rising trend in oesophageal adenocarcinoma. *Int. J. Cancer* **102**: 422, 2002.
 18. Overholt, B. F., Panjehpour, M., and Halberg, D. L. Photodynamic therapy for Barrett's esophagus with dysplasia and/or early stage carcinoma: Long-term results. *Gastrointest. Endosc.* **58**: 183, 2003.
 19. Pacifico, R. J., and Wang, K. K. Nonsurgical management of Barrett's esophagus with high-grade dysplasia. *Surg. Oncol. Clin. North Am.* **11**: 321, 2002.
 20. Buttar, N. S., Wang, K. K., Lutzke, L. S., et al. Combined endoscopic mucosal resection and photodynamic therapy for esophageal neoplasia within Barrett's esophagus. *Gastrointest. Endosc.* **54**: 682, 2001.
 21. Wolfsen, H. C., Hemminger, L. L., Raimondo, M., and Woodward, T. A. Photodynamic therapy and endoscopic mucosal resection for Barrett's dysplasia and early esophageal adenocarcinoma. *South Med. J.* **97**: 827, 2004.
 22. Giovannini, M., Bories, E., Pesenti, C., et al. Circumferential endoscopic mucosal resection in Barrett's esophagus with high-grade intraepithelial neoplasia or mucosal cancer. Preliminary results in 21 patients. *Endoscopy* **36**: 782, 2004.
 23. Katada, C., Muto, M., Manabe, T., et al. Esophageal stenosis after endoscopic mucosal resection of superficial esophageal lesions. *Gastrointest. Endosc.* **57**: 165, 2003.
 24. Fitzgerald, R. C. Ablative mucosectomy is the procedure of choice to prevent Barrett's cancer. *Gut* **52**: 16, 2003.
 25. Luman, W., Lessels, A. M., and Palmer, K. R. Failure of Nd-YAG photocoagulation therapy as treatment for Barrett's oesophagus: A pilot study. *Eur. J. Gastroenterol. Hepatol.* **8**: 627, 1996.
 26. Sharma, P., Bhattacharyya, A., Garewal, H. S., and Sampliner, R. E. Durability of new squamous epithelium after endoscopic reversal of Barrett's esophagus. *Gastrointest. Endosc.* **50**: 159, 1999.
 27. Hayashi, K., Ando, N., Ozawa, S., et al. A neo-esophagus reconstructed by cultured human esophageal epithelial cells, smooth muscle cells, fibroblasts, and collagen. *Asaio. J.* **50**: 261, 2004.
 28. Sato, M., Ando, N., Ozawa, S., et al. An artificial esophagus consisting of cultured human esophageal epithelial cells, polyglycolic acid mesh, and collagen. *Asaio. J.* **40**: M389, 1994.
 29. Sato, M., Ando, N., Ozawa, S., et al. A hybrid artificial esophagus using cultured human esophageal epithelial cells. *Asaio. J.* **39**: M554, 1993.
 30. Kropp, B. P., Eppley, B. L., Prevel, C. D., et al. Experimental assessment of small intestinal submucosa as a bladder wall substitute. *Urology* **46**: 396, 1995.
 31. Kropp, B. P., Rippey, M. K., Badylak, S. F., et al. Regenerative urinary bladder augmentation using small intestinal submucosa: Urodynamic and histopathologic assessment in long-term canine bladder augmentations. *J. Urol.* **155**: 2098, 1996.
 32. Sievert, K. D., and Tanagho, E. A. Organ-specific acellular matrix for reconstruction of the urinary tract. *World J. Urol.* **18**: 19, 2000.
 33. Yoo, J. J., Meng, J., Oberpenning, F., and Atala, A. Bladder augmentation using allogenic bladder submucosa seeded with cells. *Urology* **51**: 221, 1998.
 34. Sandusky, G. E., Jr., Badylak, S. F., Morff, R. J., et al. Histologic findings after in vivo placement of small intestine submucosal vascular grafts and saphenous vein grafts in the carotid artery in dogs. *Am. J. Pathol.* **140**: 317, 1992.
 35. Sandusky, G. E., Lantz, G. C., and Badylak, S. F. Healing comparison of small intestine submucosa and ePTFE grafts in the canine carotid artery. *J. Surg. Res.* **58**: 415, 1995.
 36. Schoder, M., Pavcnik, D., Uchida, B. T., et al. Small intestinal submucosa aneurysm sac embolization for endoleak prevention after abdominal aortic aneurysm endografting: A pilot study in sheep. *J. Vasc. Interv. Radiol.* **15**: 69, 2004.
 37. MacLeod, T. M., Sarathchandra, P., Williams, G., et al. Evaluation of a porcine origin acellular dermal matrix and small intestinal submucosa as dermal replacements in preventing secondary skin graft contraction. *Burns* **30**: 431, 2004.
 38. Prevel, C. D., Eppley, B. L., Summerlin, D. J., et al. Small intestinal submucosa: Utilization as a wound dressing in full-thickness rodent wounds. *Ann. Plast. Surg.* **35**: 381, 1995.
 39. Badylak, S. F., Tullius, R., Kokini, K., et al. The use of xenogeneic small intestinal submucosa as a biomaterial for Achilles tendon repair in a dog model. *J. Biomed. Mater. Res.* **29**: 977, 1995.
 40. Dejardin, L. M., Arnoczky, S. P., Ewers, B. J., et al. Tissue-engineered rotator cuff tendon using porcine small intestinal submucosa. Histologic and mechanical evaluation in dogs. *Am. J. Sports Med.* **29**: 175, 2001.
 41. Badylak, S., Meurling, S., Chen, M., et al. Resorbable bioscaffold for esophageal repair in a dog model. *J. Pediatr. Surg.* **35**: 1097, 2000.
 42. Brant, A. M., Shah, S. S., Rodgers, V. G., et al. Biomechanics of the arterial wall under simulated flow conditions. *J. Biomech.* **21**: 107, 1988.
 43. Jankowski, R. J., Prantil, R. L., Fraser, M. O., et al. Development of an experimental system for the study of urethral biomechanical function. *Am. J. Physiol. Renal. Physiol.* **286**: F225, 2004.
 44. Labadie, R. F., Antaki, J. F., Williams, J. L., et al. Pulsatile perfusion system for ex vivo investigation of biochemical pathways in intact vascular tissue. *Am. J. Physiol.* **270**: H760, 1996.
 45. Raghavan, M. L., Webster, M. W., and Vorp, D. A. Ex vivo biomechanical behavior of abdominal aortic aneurysm: Assessment using a new mathematical model. *Ann. Biomed. Eng.* **24**: 573, 1996.
 46. Vorp, D. A., Schiro, B. J., Ehrlich, M. P., et al. Effect of aneurysm on the tensile strength and biomechanical behavior of the ascending thoracic aorta. *Ann. Thorac. Surg.* **75**: 1210, 2003.
 47. Atala, A. Engineering tissues and organs. *Curr. Opin. Urol.* **9**: 517, 1999.
 48. Atala, A. Creation of bladder tissue in vitro and in vivo. A system for organ replacement. *Adv. Exp. Med. Biol.* **462**: 31, 1999.
 49. Yoo, J. J., and Atala, A. Tissue engineering applications in the genitourinary tract system. *Yonsei. Med. J.* **41**: 789, 2000.
 50. Atala, A. Tissue engineering in urology. *Curr. Urol. Rep.* **2**: 83, 2001.
 51. Kropp, B. P., Cheng, E. Y., Pope, J. Ct., et al. Use of small intestinal submucosa for corporal body grafting in cases of severe penile curvature. *J. Urol.* **168**: 1742, 2002; discussion 1745.
 52. Strange, P. S. Small intestinal submucosa for laparoscopic repair of large paraesophageal hiatal hernias: A preliminary report. *Surg. Technol. Int.* **11**: 141, 2003.
 53. Badylak, S., Kokini, K., Tullius, B., et al. Morphologic study of small intestinal submucosa as a body wall repair device. *J. Surg. Res.* **103**: 190, 2002.
 54. Badylak, S., Kokini, K., Tullius, B., and Whitson, B. Strength over time of a resorbable bioscaffold for body wall repair in a dog model. *J. Surg. Res.* **99**: 282, 2001.
 55. *Methods of Tissue Engineering*, pp 505–514. San Diego, Academic Press, 2000.
 56. Master, V. A., Wei, G., Liu, W., and Baskin, L. S. Urothelium

- facilitates the recruitment and trans-differentiation of fibroblasts into smooth muscle in acellular matrix. *J. Urol.* **170**: 1628, 2003.
57. Vaught, J. D., Kropp, B. P., Sawyer, B. D., *et al.* Detrusor regeneration in the rat using porcine small intestinal submucosal grafts: Functional innervation and receptor expression. *J. Urol.* **155**: 374, 1996.
 58. Chen, F., Yoo, J. J., and Atala, A. Acellular collagen matrix as a possible "off the shelf" biomaterial for urethral repair. *Urology* **54**: 407, 1999.
 59. Price, R. D., Das-Gupta, V., Frame, J. D., and Navsaria, H. A. A study to evaluate primary dressings for the application of cultured keratinocytes. *Br. J. Plast. Surg.* **54**: 687, 2001.
 60. Kipshidze, N., Dangas, G., Tsapenko, M., *et al.* Role of the endothelium in modulating neointimal formation: Vasculoprotective approaches to attenuate restenosis after percutaneous coronary interventions. *J. Am. Coll. Cardiol.* **44**: 733, 2004.
 61. Vouyouka, A. G., Jiang, Y., and Basson, M. D. Pressure alters endothelial effects upon vascular smooth muscle cells by decreasing smooth muscle cell proliferation and increasing smooth muscle cell apoptosis. *Surgery* **136**: 282, 2004.
 62. Rheinwald, J. G., and Green, H. Serial cultivation of strains of human epidermal keratinocytes: The formation of keratinizing colonies from single cells. *Cell* **6**: 331, 1975.
 63. Hillegonds, D. J., Record, R., Rickey, F. A., *et al.* Prime lab sample handling and data analysis for accelerator-based biomedical radiocarbon analysis. *Radiocarbon.* **43**: 305, 2001.
 64. Record, R. D., Hillegonds, D., Simmons, C., *et al.* In vivo degradation of ¹⁴C-labeled small intestinal submucosa (SIS) when used for urinary bladder repair. *Biomaterials* **22**: 2653, 2001.
 65. Rickey, F. A., Elmore, D., Hillegonds, D., *et al.* Re-generation of tissue about an animal-based scaffold: AMS studies of the fate of the scaffold. *Nucl. Instr. Meth. Phys. Res.* **172**: 904, 2000.
 66. Badylak, S. F., Park, K., Peppas, N., *et al.* Marrow-derived cells populate scaffolds composed of xenogeneic extracellular matrix. *Exp. Hematol.* **29**: 1310, 2001.
 67. Li, F., Li, W., Johnson, S., *et al.* Low-molecular-weight peptides derived from extracellular matrix as chemoattractants for primary endothelial cells. *Endothelium* **11**: 199, 2004.